Journal of Cardiology (2010) **55**, 23—33

ScienceDirect

journal homepage: www.elsevier.com/locate/jjcc

ORIGINAL ARTICLE

Concentric left ventricular hypertrophy brings deterioration of systolic longitudinal, circumferential, and radial myocardial deformation in hypertensive patients with preserved left ventricular pump function

Yukio Mizuguchi (MD)*, Yoshifumi Oishi (MD, FJCC), Hirokazu Miyoshi (MD), Arata Iuchi (MD, FJCC), Norio Nagase (MD), Takashi Oki (MD, FJCC)

Cardiovascular Section, Higashi Tokushima National Hospital, National Hospital Organization, 1-1 Ohmukai-kita, Ohtera, Itano, Tokushima 779-0193, Japan

Received 14 May 2009; received in revised form 22 July 2009; accepted 23 July 2009
Available online 2 September 2009

KEYWORDS
2D strain imaging;
LV hypertrophy;
LV systolic myocardial deformation;
Isolated diastolic heart failure

Summary
Background: We hypothesized that deterioration of systolic left ventricular (LV) myocardial deformation exists as an early sign of ''isolated'' diastolic heart failure in patients with hypertension (HT) and LV hypertrophy (LVH).
Methods and results: Two-dimensional strain echocardiography was performed in 98 patients with HT and 22 age-matched normal controls. The LV mass index and relative wall thickness were used to assign patients into 3 groups with normal geometry (N-LV, $n=31$), concentric hypertrophy (C-LVH, $n=25$), and eccentric hypertrophy (E-LVH, $n=42$). The LV ejection fraction was preserved ($\geq$50%) in the 3 HT groups. The mean peak systolic longitudinal, circumferential, and radial strains in the C-LVH group were lower compared to the control and other 2 HT groups. The mean peak systolic strain rates in the 3 directions in the C-LVH group and those in the longitudinal and radial directions in the E-LVH and N-LV groups were lower compared to the control group. In addition, the mean peak systolic circumferential strain rate was lower in the C-LVH group than in the other 2 HT groups. There were no differences in the LV torsion and torsional rate between the control and 3 HT groups. The mean peak systolic circumferential strain was an independent predictor related to LV ejection fraction in all patients.

* Corresponding author. Tel.: +81 88 672 2912; fax: +81 88 672 3809.
E-mail address: mizuguchi@higasitokusima.hosp.go.jp (Y. Mizuguchi).

0914-5087/$ — see front matter
doi:10.1016/j.jjcc.2009.07.006

Conclusions: C-LVH caused deterioration of the systolic longitudinal, circumferential, and radial myocardial deformation in patients with HT. LV torsion and circumferential shortening were considered to be compensatory mechanisms for maintaining LV pump function.

Introduction

Hypertension (HT) causes left ventricular (LV) systolic pressure overload due to an increase in peripheral vascular resistance. As a result, various LV geometric changes are present in this disease [1], which progresses to diastolic dysfunction with or without symptoms of heart failure (HF) and/or HF with systolic dysfunction. According to the Framingham study, LV hypertrophy (LVH) is an established risk factor in myocardial infarction and cardiovascular mortality [2]. Furthermore, association between HT with LVH and deterioration to isolated diastolic HF is well recognized [3,4]. It has been reported that longitudinal LV shortening is first impaired in elderly normal individuals [5] and in patients with hypertrophic cardiomyopathy and preserved LV ejection fraction [6]. Therefore, it is clinically important to accurately evaluate not only LV diastolic function but also mechanics of LV myocardial contraction in patients with HT and LVH. Recently, the development of two-dimensional (2D) strain imaging has facilitated the simple and angle-independent measurement of LV myocardial deformation in the longitudinal, circumferential, and radial directions [7–9]. In the present study, we recorded regional LV myocardial strain and strain rate curves in the 3 directions and LV torsion and torsion rate curves in patients with HT using 2D strain imaging, and investigated features of LV myocardial three-dimensional contraction abnormalities in the presence of LVH, particularly concentric hypertrophy, to speculate the background of isolated diastolic heart failure.

Methods

Patient selection

The study included 98 consecutive HT patients from an outpatient clinic population. All patients fulfilled the following criteria: (1) systolic blood pressure (BP) $\geq$140 mmHg, diastolic BP $\geq$90 mmHg, or both, on 2 or more hospital visits at one-week intervals before treatment with antihypertensive medication; (2) continued treatment for $\leq$2 months after providing formal informed consent; (3) no clinical, laboratory, or echocardiographic evidence of congestive heart failure, coronary heart disease, atrial fibrillation, previous stroke, significant valvular disease, secondary causes of hypertension, diabetes mellitus, or important concomitant disease; (4) LV ejection fraction $\geq$50%; (5) good-quality echocardiographic recordings.

A total of 22 age-matched controls were selected from 65 subjects presenting with symptoms of chest pain, palpitations, dyspnea, or heart murmurs in whom clinical and laboratory examinations, phonocardiography, conventional echocardiography, and exercise testing were normal. All patients gave written informed consent, and the study was approved by the ethics committee of the institution involved.

Conventional, pulsed Doppler, and tissue Doppler echocardiography

All echocardiographic measurements were performed using a commercially available ultrasound system (Vivid 7, General Electric Healthcare, Milwaukee, WI, USA) equipped with a harmonic 4.0-MHz variable-frequency phased-array transducer. The end-diastolic LV diameter (Dd), end-systolic LV diameter (Ds), end-diastolic thickness of the ventricular septum (VSth), and end-diastolic thickness of the LV posterior wall (PWth) were measured by M-mode echocardiography. By using these parameters, we calculated the LV mass [10] and relative LV wall thickness as follows:

$$\text{LV mass (g)} = 0.8 \times 1.04 \times [(\text{Dd} + \text{PWth} + \text{VSth})^3 - \text{Dd}^3] + 0.6$$

$$\text{Relative LV wall thickness} = 2 \times \frac{\text{PWth}}{\text{Dd}}$$

The LV mass index (g/m^2) was determined by dividing the LV mass measurement by the body surface area.

In all 98 patients, LV mass was classified as normal geometry (N-LV) in 31 patients (LV mass index $\leq$115 g/m^2 for men and $\leq$95 g/m^2 for women, and relative LV wall thickness $\leq$0.42), concentric LVH (C-LVH) in 25 patients (LV mass index >115 g/m^2 for men and >95 g/m^2 for women, and relative LV wall thickness >0.42), and eccentric LVH (E-LVH) in 42 patients (LV mass index >115 g/m^2 for men and >95 g/m^2 for women, and relative LV wall thickness <0.42).

The LV end-diastolic volume (EDV) and end-systolic volume (ESV) were calculated from the apical 2- and 4-chamber views using a modified Simpson's method. The LV ejection fraction was calculated as ejection fraction = (EDV − ESV)/EDV × 100. Left atrial volume was measured offline using the biplane area-length method, and was indexed to the body surface area.

The peak early diastolic velocity (*E*), the deceleration time from the peak of the early diastolic wave to baseline (E-DT), the peak atrial systolic velocity (*A*), and the *E*/*A* ratio were assessed from the transmitral flow velocity pattern.

The transmitral flow and LV outflow velocity patterns were obtained from the apical long-axis view with the pulsed Doppler method. The Tei index was calculated as follows: Tei index = $(a - b)/a$, where a is the interval between cessation and onset of transmitral flow, and b is the ejection time of LV outflow.

The mitral annular motion velocity was recorded at the LV posterior wall site in the apical LV long-axis view by pulsed tissue Doppler echocardiography. The peak systolic motion

velocity (s'), peak early diastolic motion velocity (e'), peak motion velocity during atrial systole (a'), and ratio of peak early diastolic transmitral flow velocity (E) to e' (E/e') were determined [11].

Two-dimensional strain imaging

We acquired LV short-axis views at the apical, mid, and basal levels, and LV apical 2- and 4-chamber views using a high frame rate (65—69 frames/s). The basal short-axis view contained the mitral valve, the mid-short-axis view contained the chordae tendineae, and the apical short-axis view was acquired distal to the papillary muscles. At each plane, 3 consecutive cardiac cycles were acquired at end-expiration breath holding and stored digitally on a hard disk for offline analysis. Image analysis was performed offline on a PC workstation using custom analysis software (Echopac PC, Version 6.0.X, GE Healthcare, Fairfield, CT, USA). The LV endocardial border of the end-systolic frame was manually traced. On the basis of this line, the computer automatically created a region of interest including the entire transmural wall in all patients, and the software selected natural acoustic markers moving with the tissue. Automatic frame-by-frame tracking of these markers during the cardiac cycle (2D systolic time interval method) yielded a measure of rotation, rotational velocity, strain, and strain rate at any point of myocardium. The LV was divided into 18 segments, and each segment was individually analyzed. With the use of a dedicated software package, 2D LV strain, strain rate, and rotation were measured as previously described [7].

In the present study, longitudinal strain and strain rate were assessed in the 6 LV walls on the apical 2-chamber view and in the 6 LV walls on the apical 4-chamber view, and their average values were used for comparisons among the control, and 3 HT groups (Fig. 1). Circumferential strain and strain rate were assessed in the 6 LV walls on the parasternal LV short-axis view at the level of the chordae tendineae, and their average values were used for comparison. Radial strain and strain rate were assessed in the 6 LV walls on the parasternal LV short-axis view at the level of the chordae tendineae, and each value was used for the comparison.

LV rotation and torsion along the long-axis were assessed using parasternal LV short-axis views at the basal level, including the mitral valves, and at the apical level excluding the papillary muscles. An effort was made to make both of the LV short-axis sections as circular as possible. When viewed from the LV apex, the systolic rotation of the base was clockwise and is expressed as a negative value, whereas the rotation of the apex was counterclockwise and

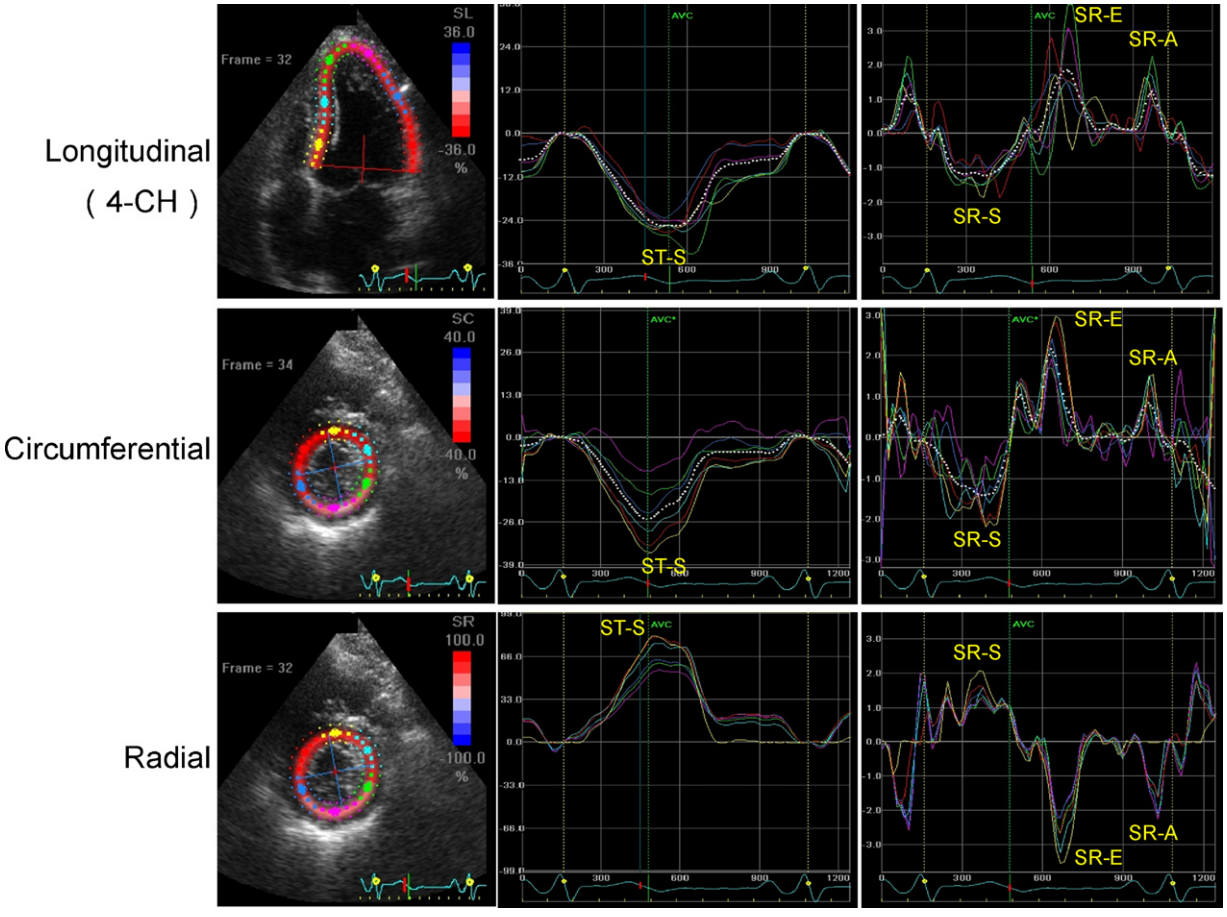

Figure 1 Longitudinal, circumferential, and radial strain and strain rate curves of left ventricular walls using two-dimensional speckle-tracking imaging in a healthy subject. 4-CH, apical 4-chamber view; ST-S, peak systolic strain; SR-S, peak systolic strain rate; SR-E, peak early diastolic strain rate; SR-A, peak strain rate during atrial systole.

Table 1 Comparisons of clinical parameters among 4 groups.

	Control ($n=22$)	C-LVH ($n=25$)	E-LVH ($n=42$)	N-LV ($n=31$)
Age (yrs)	59 ± 12	62 ± 10	64 ± 9	62 ± 13
Gender (men/women)	7/15	16/9	25/17	19/12
Height (cm)	156 ± 7.6	159 ± 8.7	158 ± 8.8	159 ± 8.9
Weight (kg)	54 ± 8.9	65 ± 15.1$^{\int\int}$	61 ± 10.5$^{\int}$	61 ± 10.2$^{\int}$
BMI (kg/m^2)	21.9 ± 3.0	25.2 ± 4.4$^{\int\int}$	24.4 ± 3.1$^{\int\int}$	24.1 ± 2.9$^{\int}$
BSA (m^2)	1.5 ± 0.2	1.7 ± 0.2$^{\int}$	1.6 ± 0.2	1.6 ± 0.2
Medications				
ARBs ($n=74$)	0	17	33	24
β-Blockers ($n=1$)	0	0	1	0
Diuretics ($n=7$)	0	5	2	0
CCBs ($n=16$)	0	3	8	5
SBP (mmHg)	119 ± 11	140 ± 17$^{\int\int}$	135 ± 23$^{\int\int}$	131 ± 11$^{\int}$
DBP (mmHg)	70 ± 8	80 ± 12$^{\int\int,\dagger}$	74 ± 11	76 ± 9
PP (mmHg)	46 ± 11	58 ± 14$^{\int}$	61 ± 19$^{\int\int}$	55 ± 12
Heart rate (beats/min)	70 ± 9	64 ± 8	63 ± 10$^{\int}$	67 ± 9

C-LVH, concentric hypertrophy; E-LVH, eccentric hypertrophy; N-LV, normal geometry; BMI, body mass index; BSA, body surface area; ARBs, angiotensin receptor blockers; CCBs, calcium channel blockers; SBP, systolic blood pressure; DBP, diastolic blood pressure; PP, pulse pressure.
$^{\int}$ $P<0.05$.
$^{\int\int}$ $P<0.01$ vs control group.
† $P<0.05$ vs E-LVH group.

is expressed as a positive value. Therefore, torsion is defined as the difference between the apical and basal rotation, and was divided by end-diastolic LV longitudinal length between the LV apex and the mitral plane [12,13]. We recorded LV rotation and rotational velocity profiles during a cardiac cycle at the base and apex using the software package described above. Data points representing the basal and apical LV rotation and rotational velocity were exported to a spreadsheet program (Microsoft Excel, Microsoft Corp, Redmond, WA, USA) to create LV torsion and torsion rate profiles. All variables in this study represent the mean value of measurements taken in 3 consecutive cardiac cycles.

Statistical analysis

Values are expressed as the mean ± standard deviation. Comparison of variables between the 4 groups was performed using analysis of variance. Post hoc analysis was done using the Bonferroni method. The significance of correlations between the mitral annular motion velocity and LV strain parameters and the LV ejection fraction and LVMI were determined by linear regression analysis. Multivariable regression analysis was applied to evaluate the relationships between the LV ejection fraction and LVMI and other continuous variables. A P value less than 0.05 was considered statistically significant.

Results

Clinical characteristics

The body weight, body mass index (BMI), and systolic blood pressure were greater in the 3 HT groups than in the control group (Table 1). Also, diastolic blood pressure was greater in the C-LVH group compared to the control and E-LVH groups.

M-mode, two-dimensional, and pulsed Doppler echocardiography

The end-diastolic LV diameter was greater in the E-LVH group than in the other 3 groups (Table 2). The indexed LA volumes in the C-LVH and E-LVH groups were greater compared to the control and N-LV groups. The end-diastolic LV wall thicknesses in the C-LVH and E-LVH groups, particularly in the former, were greater compared to the control and N-LV groups. The relative LV wall thickness was markedly increased in the C-LVH group than in the other 3 groups. The LV mass index was greater in both LVH groups, particularly in the C-LVH group, than in the control and N-LV groups. The LV ejection fraction was lower in the C-LVH group than in the control group, whereas there were no differences among the 3 HT groups. The E/As in the 3 HT groups were lower compared to the control group, and E-DT was longer in the 2 LVH groups than in the control group. The Tei index was greater in the C-LVH group than in the control and N-LV groups.

Tissue Doppler echocardiography

The peak systolic and early diastolic mitral annular motion velocities (s' and e', respectively) were lower in the C-LVH group than in the control and other 2 HT groups (Table 3). The E/e' was greater in the C-LVH group than in the other 3 groups. The LV ejection fraction correlated with s' and a', and LVMI correlated with s', e', and E/e' in all patients (Table 4).

Table 2 Comparisons of M-mode, two-dimensional, and pulsed Doppler echocardiographic parameters among 4 groups.

	Control ($n = 22$)	C-LVH ($n = 25$)	E-LVH ($n = 42$)	N-LV ($n = 31$)
End-diastolic LV diameter (cm)	4.8 ± 0.4	4.8 ± 0.3†††	5.3 ± 0.5$^{\int\int\int,***}$	4.9 ± 0.4
End-systolic LV diameter (cm)	2.6 ± 0.4	2.8 ± 0.6	3.0 ± 0.5$^{\int}$	2.8 ± 0.5
LA volume/BSA (ml/m^2)	20.9 ± 9.9	30.6 ± 11.3$^{\int\int,*}$	30.1 ± 10.4$^{\int\int\int,*}$	24.2 ± 7.0
End-diastolic ventricular septal thickness (mm)	7.8 ± 1.1	11.9 ± 1.5$^{\int\int\int,***,\dagger\dagger\dagger}$	9.6 ± 1.1$^{\int\int\int,***}$	7.5 ± 1.2
End-diastolic LV posterior wall thickness (mm)	8.1 ± 1.2	11.7 ± 1.4$^{\int\int\int,***,\dagger\dagger\dagger}$	9.6 ± 1.0$^{\int\int\int,***}$	7.8 ± 1.0
Relative LV wall thickness	0.34 ± 0.05	0.49 ± 0.06$^{\int\int\int,***,\dagger\dagger\dagger}$	0.37 ± 0.05***	0.32 ± 0.05
LV mass index (g/m^2)	97.2 ± 13.8	160.1 ± 37.7$^{\int\int\int,***,\dagger}$	144.0 ± 24.3$^{\int\int\int,***}$	94.4 ± 12.8
LV ejection fraction (%)	77.4 ± 8.1	70.4 ± 11.8$^{\int\int}$	73.4 ± 7.6	73.3 ± 7.7
E (cm/s)	0.76 ± 0.2	0.65 ± 0.1$^{\int,\dagger\dagger}$	0.76 ± 0.2	0.71 ± 0.2
A (cm/s)	0.67 ± 0.1	0.79 ± 0.2$^{\int}$	0.85 ± 0.2$^{\int\int\int}$	0.78 ± 0.2$^{\int}$
E/*A*	1.15 ± 0.3	0.86 ± 0.2$^{\int\int\int}$	0.92 ± 0.3$^{\int\int\int}$	0.96 ± 0.3$^{\int\int}$
E-DT (ms)	183 ± 29.8	214 ± 37.3$^{\int\int,*}$	213 ± 44.0$^{\int\int,*}$	106 ± 26.7
Tei index	0.24 ± 0.12	0.35 ± 0.13$^{\int\int,**}$	0.29 ± 0.13	0.26 ± 0.11

C-LVH, concentric hypertrophy; E-LVH, eccentric hypertrophy; N-LV, normal geometry; LV, left ventricle; LA, left atrium; BSA, body surface area; *E*, peak early diastolic velocity of transmitral flow; *A*, peak atrial systolic velocity of transmitral flow; E-DT, deceleration time from the peak to baseline of the early diastolic transmitral flow velocity.

$^{\int}$ $P < 0.05$.
$^{\int\int}$ $P < 0.01$.
$^{\int\int\int}$ $P < 0.001$ vs control group.
* $P < 0.05$.
** $P < 0.01$
*** $P < 0.001$ vs N-LV group.
† $P < 0.05$.
†† $P < 0.01$.
††† $P < 0.001$ vs E-LVH group.

Table 3 Comparisons of tissue velocity and 2D strain imaging parameters among 4 groups.

	Control ($n=22$)	C-LVH ($n=25$)	E-LVH ($n=42$)	N-LV ($n=31$)
Mitral annular motion velocity				
s'(cm/s)	10.2 ± 2.8	8.2 ± 2.3$^{\int\int,*,\dagger}$	9.5 ± 2.1	9.6 ± 2.9
e'(cm/s)	11.1 ± 3.3	7.2 ± 2.8$^{\int\int\int,***,\dagger\dagger}$	9.6 ± 2.9	10.5 ± 3.1
a'(cm/s)	10.2 ± 2.8	9.7 ± 2.4*,††	11.4 ± 2.2	11.3 ± 2.5
E/e'	7.3 ± 2.4	10.3 ± 4.1$^{\int\int,***,\dagger}$	8.5 ± 2.9	7.3 ± 2.3
LV wall strain and strain rate				
Peak systolic strain (%)				
Longitudinal	−22.9 ± 1.7	−17.9 ± 2.9$^{\int\int\int,***,\dagger\dagger\dagger}$	−20.0 ± 2.1$^{\int\int\int}$	−20.4 ± 2.7$^{\int\int\int}$
Radial	74.4 ± 8.0	62.7 ± 14.4$^{\int\int,*,\dagger}$	70.1 ± 14.4	70.2 ± 10.0
Circumferential	−23.7 ± 3.0	−20.4 ± 4.5$^{\int\int,**,\dagger}$	−21.7 ± 3.5$^{\int}$	−23.0 ± 2.9
Systolic strain rate (s^{-1})				
Longitudinal	−1.4 ± 0.2	−1.2 ± 0.3$^{\int\int\int}$	−1.2 ± 0.2$^{\int\int}$	−1.2 ± 0.2$^{\int\int}$
Radial	2.8 ± 0.6	2.2 ± 0.6$^{\int\int}$	2.4 ± 0.6$^{\int\int}$	2.4 ± 0.6$^{\int\int}$
Circumferential	−1.8 ± 0.2	−1.5 ± 0.4$^{\int\int,*,\dagger}$	−1.7 ± 0.3	−1.7 ± 0.3
Early diastolic strain rate (s^{-1})				
Longitudinal	1.8 ± 0.3	1.2 ± 0.4$^{\int\int\int,***,\dagger\dagger\dagger}$	1.5 ± 0.3$^{\int\int\int}$	1.5 ± 0.3$^{\int\int\int}$
Radial	−2.7 ± 0.9	−2.0 ± 0.7$^{\int\int}$	−2.2 ± 0.6$^{\int}$	−2.3 ± 0.6$^{\int}$
Circumferential	2.0 ± 0.4	1.6 ± 0.5$^{\int\int\int,**,\dagger}$	1.8 ± 0.3	1.9 ± 0.5
Atrial systolic strain rate (s^{-1})				
Longitudinal	1.3 ± 0.3	1.2 ± 0.3	1.2 ± 0.3	1.4 ± 0.4
Radial	−1.2 ± 0.8	−1.8 ± 0.8$^{\int}$	−1.7 ± 0.8$^{\int}$	−1.8 ± 1.0$^{\int}$
Circumferential	1.2 ± 0.3	1.2 ± 0.5	1.3 ± 0.4	1.3 ± 0.4
Torsion (°)	20.5 ± 6.5	21.0 ± 6.8	19.1 ± 6.1	17.9 ± 8.4
Torsion/LV length (°/cm)	2.74 ± 0.85	2.66 ± 0.88	2.47 ± 0.85	2.35 ± 1.10
Torsional rate (°/s)	130.8 ± 38.2	124.5 ± 43.5	113.4 ± 32.2	115.2 ± 44.3
Untwisting rate (°/s)	144.4 ± 50.8	134.6 ± 54.5	120.3 ± 38.8	113.9 ± 48.1$^{\int}$

C-LVH, concentric hypertrophy; E-LVH, eccentric hypertrophy; N-LV, normal geometry; LV, left ventricle; s', peak systolic mitral annular motion velocity; e', peak early diastolic mitral annular motion velocity; a', peak mitral annular motion velocity during atrial systole; E/e', ratio of peak early diastolic transmitral flow velocity to e'.
$^{\int}$ $P<0.05$.
$^{\int\int}$ $P<0.01$.
$^{\int\int\int}$ $P<0.001$ vs control group.
* $P<0.05$.
** $P<0.01$.
*** $P<0.001$ vs N-LV group.
† $P<0.05$.
†† $P<0.01$.
††† $P<0.001$ vs E-LVH group.

Two-dimensional strain imaging

In the C-LVH group, the mean peak systolic strains in the longitudinal, circumferential, and radial directions were lower compared to the other 3 groups (Table 3). The mean peak systolic longitudinal and circumferential strains were lower in the E-LVH group, and mean peak systolic longitudinal strain was lower in the N-LV group, than in the control group. In the C-LVH group, the mean peak systolic strain rates in all the 3 directions were lower compared to the control group. Also, the mean peak systolic circumferential strain rate in the C-LVH group was lower than that in the other 2 HT groups. The mean peak systolic longitudinal and radial strain rates were lower in the E-LVH and N-LV groups than in the control group. The mean peak early diastolic strain rates in all the 3 directions were lower in the C-LVH group, and those in the longitudinal and radial directions were lower in the E-LVH and N-LV groups, than in the control group. The mean peak atrial systolic radial strain rates in the 3 HT groups were greater compared to the control group. There were no differences in the torsion and torsional rate among the 4 groups. Untwisting rate was lower in the N-LV group than in the control group, whereas there were no differences between the control and 2 LVH groups.

The LV ejection fraction correlated with mean peak systolic strain and strain rate, and mean peak early diastolic and atrial systolic strain rates in the longitudinal and circumferential directions, torsion, torsional rate and untwisting rate in all patients (Table 4). The LVMI correlated with s', e', E/e', mean peak systolic strains and strain rates, mean peak early diastolic strain rates in all 3 directions, and mean peak atrial systolic longitudinal strain rate in all patients.

Table 4 Correlations between the tissue velocity and 2D strain imaging parameters and the LVEF and LVMI.

	LVEF		LVMI	
	r	*P* value	*r*	*P* value
Mitral annular motion velocity				
s′(cm/s)	0.25	<0.01	−0.28	<0.01
e′(cm/s)	0.03	NS	−0.36	<0.001
a′(cm/s)	0.29	<0.01	−0.02	NS
E/*e′*	−0.03	NS	0.42	<0.0001
LV wall strain and strain rate				
Peak systolic strain (%)				
Longitudinal	−0.38	<0.0001	0.38	<0.0001
Radial	0.15	NS	−0.34	<0.001
Circumferential	−0.60	<0.0001	0.36	<0.0001
Systolic strain rate (s^{-1})				
Longitudinal	−0.42	<0.0001	0.23	<0.05
Radial	0.18	NS	−0.30	<0.01
Circumferential	−0.54	<0.0001	0.22	<0.05
Early diastolic strain rate (s^{-1})				
Longitudinal	0.26	<0.01	−0.48	<0.0001
Radial	0.01	NS	−0.25	<0.01
Circumferential	0.34	<0.001	−0.38	<0.0001
Atrial systolic strain rate (s^{-1})				
Longitudinal	−0.41	<0.0001	−0.24	<0.05
Radial	0.01	NS	−0.07	NS
Circumferential	0.34	<0.001	−0.12	NS
Torsion (°)	0.36	<0.0001	0.07	NS
Torsion/LV length (°/cm)	0.43	<0.0001	0.04	NS
Torsional rate (°/s)	0.49	<0.0001	−0.09	NS
Untwisting rate (°/s)	−0.27	<0.01	−0.01	NS

LVEF, left ventricular ejection fraction; LVMI, left ventricular mass index; *s′*, peak systolic mitral annular motion velocity; *e′*, peak early diastolic mitral annular motion velocity; *a′*, peak mitral annular motion velocity during atrial systole; *E*/*e′*, ratio of peak early diastolic transmitral flow velocity to *e′*; LV, left ventricle; NS, not significant.

Table 5 Multivariate regression analysis to determine the best predictor of LVEF.

	β	*P* value
s′	0.135	0.1120
a′	0.020	0.8289
Peak systolic longitudinal strain	−0.057	0.6520
Peak systolic circumferential strain	−0.445	<0.0001
Peak systolic longitudinal strain rate	−0.027	0.8212
Peak systolic circumferential strain rate	0.077	0.5012
Peak early diastolic longitudinal strain rate	−0.068	0.5217
Peak early diastolic circumferential strain rate	−0.113	0.2356
Peak atrial systolic longitudinal strain rate	0.178	0.1334
Peak atrial systolic circumferential strain rate	0.050	0.5990
Torsion/LV length	0.099	0.3238
Torsional rate	0.230	0.0494
Untwisting rate	0.028	0.7515

LVEF, left ventricular ejection fraction; β, regression coefficient; *s′*, peak systolic mitral annular motion velocity; *a′*, peak mitral annular motion velocity during atrial systole; LV, left ventricle.

Table 6 Multivariate regression analysis to determine the best predictor of LVMI.

	β	*P* value
s'	0.053	0.6477
e'	−0.043	0.7929
E/e'	0.395	0.0039
Peak systolic longitudinal strain	−0.207	0.1132
Peak systolic radial strain	−0.233	0.0077
Peak systolic circumferential strain	0.345	0.0030
Peak systolic longitudinal strain rate	0.184	0.1393
Peak systolic radial strain rate	−0.202	0.0239
Peak systolic circumferential strain rate	−0.402	0.0011
Peak early diastolic longitudinal strain rate	−0.189	0.1660
Peak early diastolic radial strain rate	−0.008	0.9315
Peak early diastolic circumferential strain rate	−0.072	0.5293
Peak atrial systolic longitudinal strain rate	−0.290	0.0095

LVMI, left ventricular mass index; β, regression coefficient; s', peak systolic mitral annular motion velocity; e', peak early diastolic mitral annular motion velocity; E/e', ratio of peak early diastolic transmitral flow velocity to e'.

Multivariate regression analyses suggested that peak systolic circumferential strain and torsional rate, particularly the former, were identified as independent predictors related to LV ejection fraction (Table 5), and that E/e', peak systolic radial and circumferential strain, and peak systolic radial, circumferential and atrial systolic strain rates were identified as independent predictors related to LVMI (Table 6).

Reproducibility

Intraobserver and interobserver variabilities were assessed for velocity, strain, and torsion and untwisting values. Variability was expressed as the coefficient of variation. The intraobserver variability was 2.6—4.0% for velocity values, 4.5—5.8% for strain values, and 4.4—7.5% for torsion and untwisting values. The interobserver variability was 4.2—6.5% for velocity values, 5.6—7.5% for strain values, and 6.0—8.0% for torsion and untwisting values.

Discussion

Risk factors for isolated diastolic HF include advanced age, female gender, and HT [3,4,14,15]. Therefore, it is clinically important to accurately evaluate the relationship between LV geometry [1] and LV myocardial contractility [8,9,16] in patients with HT.

The LV myocardium consists of circumferential fibers in the mid-wall layer and longitudinal fibers in the endocardial and epicardial layers, and myofiber orientation changes continuously from right-handed helix in subendocardium to left-handed helix in subepicardium [17]. LV function is determined by the sum of contraction and relaxation in these 3 layers [18,19]. It may be indispensable to evaluate LV myocardial contractility, even when the LV ejection fraction is maintained, for clarifying the pathogenesis of isolated diastolic heart failure.

The radial wall thickening and longitudinal torsion may play an important role in blood ejection from the LV to the aorta. Recently, the development of 2D strain imaging, in which angle-independent strain measurement is possible, has facilitated the rapid and detailed evaluation of regional LV myocardial shortening or lengthening in the longitudinal and circumferential directions, and thickening or thinning in the radial direction [7—9], and longitudinal LV torsion or untwisting [20,21].

In the present study, we clarified systolic LV dysfunction in patients with HT and LVH, particularly with concentric hypertrophy, by investigating LV myocardial deformation in 3 directions and longitudinal torsion, and concluded that this disease condition is not considered to have pure or isolated diastolic dysfunction.

Longitudinal LV function

A previous study indicated the physiologic impairment of longitudinal myocardial contractility at the isovolumic contraction with healthy aging [5]. It has also been reported that longitudinal LV contractility was decreased in patients with HT [22], diabetes [23], hypertrophic cardiomyopathy [6], or diastolic heart failure [24]. As the longitudinal myocardial velocity at the isovolumic contraction is closely related to max dP/dt [25], it was emphasized that pure or isolated diastolic dysfunction is not common in healthy elderly subjects [5] or patients with LV diastolic dysfunction [26].

The normal aging process promotes fibrosis of the subendocardial myocardium [27]. In addition, the connective tissue content increases in patients with HT and LVH [28]. On the other hand, it is well known that myocardial fibrosis related to pressure overload appears frequently in the subendocardial layer [29], and that there is a negative correlation between longitudinal myocardial velocity and the interstitial fibrosis content [30]. Based on these findings, we can conclude that longitudinal LV systolic function is deteriorated in healthy elderly subjects and patients with HT, regardless of the presence or absence of LVH.

Radial myocardial thickening

It is generally known that radial LV wall thickening is closely associated with LV pump function, and that the radial func-

tion is still maintained even when the longitudinal function is deteriorated [31,32]. A recent study using 2D strain imaging reported that longitudinal LV systolic function is first impaired in subclinical patients with cardiovascular risk factors and preserved LV pump function, and radial thickening is preserved, with an increase in circumferential shortening accompanying the decrease in longitudinal shortening, resulting in maintenance of LV ejection fraction [9]. Wang et al. [8] indicated that normal circumferential strain and torsion contribute to a preserved LV ejection fraction in patients with diastolic heart failure, although longitudinal and radial strains are deteriorated.

In the present study, systolic longitudinal strain and strain rate were significantly lower in all HT groups than in the control group. In addition, in the C-LVH group, systolic strains and strain rates in all 3 directions were significantly lower compared to the control group, and systolic strains in the 3 directions and systolic circumferential strain rate were significantly lower compared to the other 2 HT groups. Also, it was confirmed that the most important factor determining the LV ejection fraction is systolic circumferential strain.

Some studies emphasized that mid-wall fractional shortening is decreased in patients with LVH even when the LV ejection fraction is normal [33,34], and correlates closely with the systolic circumferential strain determined using 2D strain imaging [35]. Therefore, a compensatory increase in circumferential shortening may be essential for maintaining the LV ejection fraction, even in the presence of a decrease in the longitudinal shortening [9].

LV torsion

In addition to radial myocardial thickening, longitudinal LV torsion plays an important role in LV ejection. According to previous studies, an increase in LV myocardial contractility [36], physiologic aging [37], and LVH [38] enhance LV torsion, although LV systolic dysfunction [39] decreases LV torsion. However, other studies emphasized that LV torsion is unlikely to be altered by advancing age [40], pericardial defects cause a lack of LV torsion while maintaining LV regional myocardial function [41], and hypertorsion may be a sensitive early marker of diastolic dysfunction [42].

Torsion depends on the relative contractility of the subendocardial and subepicardial myocardium [13,18,43,44]. As a result, torsion is influenced by many factors, such as a decrease in the coronary flow reserve in the subendocardial myocardium [45], relative difference in torque between the subendocardial and subepicardial sides of the LV wall [37,38], and LV longitudinal length-related changes related to the apical and basal rotation [46], in patients with HT and LVH. Therefore, many complicated factors must be considered in the assessment of clinical significance of torsion.

In the present study, the LV ejection fraction in the C-LVH group was maintained, although it was significantly lower compared to the control group, despite deterioration in myocardial shortening or thickening in all 3 directions; therefore, normal LV torsion may function as a compensatory mechanism. The patient population of the present study included fairly mild grades of LV diastolic stiffness even in patients with C-LVH (E/e': 10.3 ± 4.1). Further analysis should be explored to determine the LV systolic function in patients with more stiffened LV.

Study limitations

In the present study, myocardial strain in each direction was calculated as the mean value between the subendocardium and subepicardium. Essentially, it is important to separately examine the subendocardial and subepicardial layers, for evaluating longitudinal shortening and LV torsion. Some studies reported that tissue Doppler and strain imaging are influenced by the loading conditions such as afterload [47,48]. The influence of afterload was considerably eliminated by antihypertensive medication for 2 months or less in patients with HT enrolled in the present study, although there was a significant difference in blood pressure compared to the control group.

Conclusions

The systolic LV myocardial deformation was impaired in all the longitudinal, circumferential, and radial directions in patients with HT and concentric hypertrophy, whereas LV torsion was preserved. In addition, the peak systolic circumferential strain was an independent predictor related to LV ejection fraction. Accordingly, LV torsion and circumferential shortening, particularly the latter, may be major determinants for maintaining LV pump function.

References

[1] Ganau A, Devereux RB, Roman MJ, de Simone G, Pickering TG, Saba PS, Vargiu P, Simongini I, Laragh JH. Patterns of left ventricular hypertrophy and geometric remodeling in essential hypertension. J Am Coll Cardiol 1992;19:1550—8.
[2] Levy D, Garrison RJ, Savage DD, Kannel WB, Castelli WP. Prognostic implications of echocardiographically determined left ventricular mass in the Framingham Heart Study. N Engl J Med 1990;322:1561—6.
[3] Aurigemma GP, Gaasch WH. Clinical practice. Diastolic heart failure. N Engl J Med 2004;351:1097—105.
[4] Owan T, Hodge D, Herges R, Jacobsen S, Roger V, Redfield M. Trends in prevalence and outcome of heart failure with preserved ejection fraction. N Engl J Med 2006;355:251—9.
[5] Onose Y, Oki T, Mishiro Y, Yamada H, Abe M, Manabe K, Kageji Y, Tabata T, Wakatsuki T, Ito S. Influence of aging on systolic left ventricular wall motion velocities along the long and short axes in clinically normal patients determined by pulsed tissue Doppler imaging. J Am Soc Echocardiogr 1999;12:921—6.
[6] Mishiro Y, Oki T, Yamada H, Matsuoka M, Tabata T, Wakatsuki T, Ito S. Use of angiotensin II stress pulsed tissue Doppler imaging to evaluate regional left ventricular contractility in patients with hypertrophic cardiomyopathy. J Am Soc Echocardiogr 2000;13:1065—73.
[7] Leitman M, Lysyansky P, Sidenko S, Shir V, Peleg E, Binenbaum M, Kaluski E, Krakover R, Vered Z. Two-dimensional strain—a novel software for real-time quantitative echocardiographic assessment of myocardial function. J Am Soc Echocardiogr 2004;17:1021—9.
[8] Wang J, Khoury DS, Yue Y, Torre-Amione G, Nagueh SF. Preserved left ventricular twist and circumferential deformation, but depressed longitudinal and radial deformation in

patients with diastolic heart failure. Eur Heart J 2008;29: 1283—9.
[9] Mizuguchi Y, Oishi Y, Miyoshi H, Iuchi A, Nagase N, Oki T. The functional role of longitudinal, circumferential, and radial myocardial deformation for regulating the early impairment of left ventricular contraction and relaxation in patients with cardiovascular risk factors: a study with two-dimensional strain imaging. J Am Soc Echocardiogr 2008;21:1138—44.
[10] Lang RM, Bierig M, Devereux RB, Flachskampf FA, Foster E, Pellikka PA, Picard MH, Roman MJ, Seward J, Shanewise JS, Solomon SD, Spencer KT, Sutton MS, Stewart WJ. Recommendations for chamber quantification: a report from the American Society of Echocardiography's Guidelines and Standards Committee and the Chamber Quantification Writing Group, developed in conjunction with the European Association of Echocardiography, a branch of the European Society of Cardiology. J Am Soc Echocardiogr 2005;18: 1440—63.
[11] Nagueh SF, Middleton KJ, Kopelen HA, Zoghbi WA, Quinones MA. Doppler tissue imaging: a noninvasive technique for evaluation of left ventricular relaxation and estimation of filling pressures. J Am Coll Cardiol 1997;30:1527—33.
[12] Henson RE, Song SK, Pastorek JS, Ackerman JJH, Lorenz CH. Left ventricular torsion is equal in mice and humans. Am J Physiol 2000;278:H1117—23.
[13] Sengupta PP, Korinek J, Belohlavek M, Narula J, Vannan MA, Jahangir A, Khandheria BK. Left ventricular structure and function. Basic science for cardiac imaging. J Am Coll Cardiol 2006;48:1988—2001.
[14] Fischer M, Baessler A, Hense HW, Hengstenberg C, Muscholl M, Holmer S, Döring A, Broeckel U, Riegger G, Schunkert H. Prevalence of left ventricular diastolic dysfunction in the community. Results from a Doppler echocardiographic-based survey of a population sample. Eur Heart J 2003;24:320—8.
[15] Lim Y-J, Yamamoto K, Ichikawa M, Iwata A, Hayashi T, Nakata T, Masuyama T, Mishima M. Elevation of the ratio of transmitral E velocity to early diastolic mitral annular velocity continues even after recovery from acute stage in patients with diastolic heart failure. J Cardiol 2008;52:254—60.
[16] Kono M, Kisanuki A, Takasaki K, Nakashiki K, Yuasa T, Kuwahara E, Mizukami N, Uemura T, Kubota K, Ueya N, Miyata M, Tei C. Left ventricular systolic function is abnormal in diastolic heart failure: re-assessment of systolic function using cardiac time interval analysis. J Cardiol 2009;53:437—46.
[17] Sengupta PP, Krishnamoorthy VK, Korineck J, Narula J, Vannan MA, Lester SJ, Tajik JA, Seward JB, Khandheria BK, Belohlavek M. Left ventricular form and function revisited: applied translational science to cardiovascular ultrasound imaging. J Am Soc Echocardiogr 2007;20:539—51.
[18] Streeter Jr DD, Spotnitz HM, Patel DP, Ross Jr J, Sonnenblick EH. Fiber orientation in the canine left ventricle during diastole and systole. Circ Res 1969;24:339—47.
[19] Greenbaum RA, Ho SY, Gibson DG, Becker AE, Anderson RH. Left ventricular fibre architecture in man. Br Heart J 1981;45:248—63.
[20] Notomi Y, Lysyansky P, Setser PM, Shiota T, Popovic ZB, Martin-Milklovic MG, Weaver JA, Oryszak SJ, Greenberg NL, White RD, Thomas JD. Measurement of ventricular torsion by two-dimensional ultrasound speckle tracking imaging. J Am Coll Cardiol 2005;45:2034—41.
[21] Helle-Valle T, Crosby J, Edvardsen T, Lyseggen E, Amundsen BH, Smith HJ, Rosen BD, Lima JA, Torp H, Ihlen H, Smiseth OA. New noninvasive methods for assessment of left ventricular rotation: speckle tracking echocardiography. Circulation 2005;112:3149—56.
[22] Koulouris SN, Kostopoulos KG, Triantafyllou KA, Karabinos I, Bouki TP, Karvounis HI, Omran H, Filippatos G, Kranidis I. Impaired systolic dysfunction of left ventricular longitudinal fibers: a sign of early hypertensive cardiomyopathy. Clin Cardiol 2005;28:282—6.
[23] Fang ZY, Leano R, Marwick TH. Relationship between longitudinal and radial contractility in subclinical diabetic heart disease. Clin Sci 2004;106:53—60.
[24] Yu CM, Lin H, Yang H, Kong SL, Zhang Q, Lee SWL. Progression of systolic abnormalities in patients with ''isolated'' diastolic heart failure and diastolic dysfunction. Circulation 2002;105:1195—201.
[25] Oki T, Iuchi A, Tabata T, Mishiro Y, Yamada H, Abe M, Onose Y, Wakatsuki T, Ito S. Left ventricular systolic wall motion velocities along the long and short axes measured by pulsed tissue Doppler imaging in patients with atrial fibrillation. J Am Soc Echocardiogr 1999;12:121—8.
[26] Yip GW, Zhang Y, Tan PY, Wang M, Ho PY, Brodin LA, Sanderson JE. Left ventricular long-axis changes in early diastole and systole: impact of systolic function on diastole. Clin Sci 2002;102:515—22.
[27] Lenkiewicz JE, Davies MJ, Rosen D. Collagen in human myocardium as a function of age. Cardiovasc Res 1972;6:549—55.
[28] Pearlman ES, Weber KT, Janicki JS, Pietra GG, Fishman AP. Muscle fiber orientation and connective tissue content in the hypertrophied human heart. Lab Invest 1982;46:158—64.
[29] Hittinger L, Shannon RP, Bishop SP, Gelpi RJ, Vatner SF. Subendomyocardial exhaustion of blood flow reserve and increased fibrosis in conscious dogs with heart failure. Circ Res 1989;65:971—80.
[30] Shan K, Bick RJ, Poindexter BJ, Shimoni S, Letsou GV, Reardon MJ, Howell JF, Zoghbi WA, Nagueh SF. Relation of tissue Doppler derived myocardial velocities to myocardial structure and beta-adrenergic receptor density in humans. J Am Coll Cardiol 2000;36:891—6.
[31] Vinereanu D, Nicolaides E, Tweddel AC, Madler CF, Holst B, Boden LE, Cinteza M, Rees AE, Fraser AG. Subclinical left ventricular dysfunction in asymptomatic patients with type II diabetes mellitus, related to serum lipids and glycated haemoglobin. Clin Sci 2003;105:591—9.
[32] Andersen NH, Poulsen SH, Poulsen PL, Knudsen ST, Helleberg K, Hansen KW, Berg TJ, Flyvbjerg A, Mogensen CE. Left ventricular dysfunction in hypertensive patients with type 2 diabetes mellitus. Diabet Med 2005;22:1218—25.
[33] Shimizu G, Hirota Y, Kita Y, Kawamura K, Saito T, Gaasch WH. Left ventricular midwall mechanics in systemic arterial hypertension. Myocardial function is depressed in pressure-overload hypertrophy. Circulation 1991;83:1676—84.
[34] Vinch CS, Aurigemma GP, Simon HU, Hill JC, Tighe DA, Meyer TE. Analysis of left ventricular systolic function using midwall mechanics in patients >60 years of age with hypertensive heart disease and heart failure. Am J Cardiol 2005;96:1299—303.
[35] Hurlburt HM, Aurigemma GP, Hill JC, Narayanan A, Gaasch WH, Vinch CS, Meyer TE, Tighe DA. Direct ultrasound measurement of longitudinal, circumferential, and radial strain using 2-dimensional strain imaging in normal adults. Echocardiography 2007;24:723—31.
[36] Akagawa E, Murata K, Tanaka N, Yamada H, Miura T, Kunichika H, Wada Y, Hadano Y, Tanaka T, Nose Y, Yasumoto K, Kono M, Matsuzaki M. Augmentation of left ventricular apical endocardial rotation with inotropic stimulation contributes to increased left ventricular torsion and radial strain in normal subjects. Circ J 2007;71:661—8.
[37] Takeuchi M, Nakai H, Kokumai M, Nishikage T, Otani S, Lang RM. Age-related changes in left ventricular twist assessed by two-dimensional speckle tracking imaging. J Am Soc Echocardiogr 2006;19:1077—84.
[38] Stuber M, Scheidegger MB, Fischer SE, Nagel E, Steinemann F, Hess OM, Boesiger P. Alterations in the local myocardial motion

pattern in patients suffering from pressure overload due to aortic stenosis. Circulation 1999;100:361—8.
[39] Fuchs E, Muller MF, Oswald H, Thony H, Mohacsi P, Hess OM. Cardiac rotation and relaxation in patients with chronic heart failure. Eur J Heart Fail 2004;6:715—22.
[40] Kim HK, Sohn DW, Lee SE, Choi SY, Park JS, Kim YJ, Oh BH, Park YB, Choi YS. Assessment of left ventricular rotation and torsion with two-dimensional speckle tracking echocardiography. J Am Soc Echocardiogr 2007;20:45—53.
[41] Tanaka H, Oishi Y, Mizuguchi Y, Miyoshi H, Ishimoto T, Nagase N, Yamada H, Oki T. Contribution of the pericardium to left ventricular torsion and regional myocardial function in patients with total absence of the left pericardium. J Am Soc Echocardiogr 2008;21:268—74.
[42] Park SJ, Miyazaki C, Bruce CJ, Ommen S, Miller FA, Oh JK. Left ventricular torsion by two-dimensional speckle tracking echocardiography in patients with diastolic dysfunction and normal ejection fraction. J Am Soc Echocardiogr 2008;21:1129—37.
[43] Ingels Jr NB, Hansen DE, Daughters II GT, Stinson EB, Alderman EL, Miller DC. Relation between longitudinal, circumferential, and oblique shortening and torsional deformation in the left ventricle of the transplanted human heart. Circ Res 1989;64:915—27.
[44] Ashikaga H, Coppola BA, Hopenfeld B, Leifer ES, McVeigh ER, Omens JH. Transmural dispersion of myofiber mechanics. Implications for electrical heterogeneity in vivo. J Am Coll Cardiol 2007;49:909—16.
[45] Hittinger L, Mirsky I, Shen YT, Patrick TA, Bishop SP, Vatner SF. Hemodynamic mechanisms responsible for reduced subendocardial coronary reserve in dogs with severe left ventricular hypertrophy. Circulation 1995;92:978—86.
[46] Notomi Y, Srinath G, Shiota T, Martin-Miklovic MG, Beachler L, Howell K, Ohyszak SJ, Deserranno DG, Freed AD, Greenberg NL, Younoszai A, Thomas JD. Maturational and adaptive modulation of left ventricular torsional biomechanics. Doppler tissue imaging observation from infancy to adulthood. Circulation 2006;113:2534—41.
[47] Oki T, Fukuda K, Tabata T, Mishiro Y, Yamada H, Abe M, Onose Y, Wakatsuki T, Iuchi A, Ito S. Effect of an acute increase in afterload on left ventricular regional wall motion velocity in healthy subjects. J Am Soc Echocardiogr 1999;12:476—83.
[48] Urheim S, Edvardsen T, Torp H, Angelsen B, Smiseth OA. Myocardial strain by Doppler echocardiography. Validation of a new method to quantify regional myocardial function. Circulation 2000;102:1158—64.